

1                   **Postprint: This article is accepted for publication at International Journal of Comparative**  
2                   **Psychology**

3                   Amplitude Increases of Vocalizations are Associated with Body Accelerations in Siamang  
4                   (*Sympalangus syndactylus*)

5                   Wim Pouw<sup>2</sup>, Mounia Kehy<sup>3</sup>, Marco Gamba<sup>4</sup>, Andrea Ravignani<sup>5, 6, 7</sup>

6                   1. Tilburg University, Department of Computational Cognitive Science, Tilburg University  
7                   2. Donders Institute for Brain, Cognition, and Behaviour, Radboud University Nijmegen,  
8                   Netherlands  
9                   3. Equipe de Neuro-Ethologie Sensorielle, Université Jean Monnet, France  
10                  4. Dipartimento di Scienze della Vita e Biologia dei Sistemi, Università di Torino, Torino, Italy  
11                  5. Comparative Bioacoustics Research Group, Max Planck Institute for Psycholinguistics,  
12                  Nijmegen, The Netherlands  
13                  6. Center for Music in the Brain, Department of Clinical Medicine, Aarhus University & The  
14                  Royal Academy of Music, Aarhus, Denmark  
15                  7. Department of Human Neurosciences, Sapienza University of Rome, Rome, Italy

16                  **Author note:** Correspondences can be addressed to Wim Pouw

17                  (wim.pouw@donders.ru.nl). We would like to thank the ‘Jaderpark Tier- und Freizeitpark an der  
18                  Nordsee’ for allowing us to record audiovisual data of the Siamang family at their facility. This  
19                  work has been supported by the Max Planck Institute (MPI) for Psycholinguistics Nijmegen, and  
20                  the Donders Institute for Cognition, Brain, and Behavior. We would like to thank Jeroen Geerts  
21                  of the MPI, for support of organizing the audiovisual equipment, and Maarten Snellen with his  
22                  help setting up a dedicated server to run our dashboard application. We would like to thank  
23                  Diandra Düngen for her support in making the recordings possible. WP is funded by a VENI  
24                  grant (VI.Veni 0.201G.047: PI Wim Pouw) and was further supported by a Donders Postdoctoral  
25                  Development fund. The Comparative Bioacoustics Group is supported by Max Planck  
26                  Independent Research Group Leader funding to A.R. Center for Music in the Brain is funded by  
27                  the Danish National Research Foundation (DNRF117). AR is funded by the European Union  
28                  (ERC, TOHR, 101041885). **Open data:** All data and code supporting this manuscript can be  
29                  found on [https://github.com/WimPouw/siamang\\_physical\\_constraints\\_code\\_repo](https://github.com/WimPouw/siamang_physical_constraints_code_repo)

1

2

**Abstract**

3 Siamangs (*Sympthalangus syndactylus*), one of the few singing apes, vocalize loudly, often while  
4 they move. We hypothesize that movement and vocalization coordinate, possibly due to vigorous  
5 thorax-loading movements such as brachiation affecting vocal-respiratory dynamics. To assess  
6 this vocal-motor coordination we recorded more than a hundred stereotypical vocalizations  
7 combined with movement from two captive Siamang (isolated from 7 hours of singing). We  
8 observed that stereotypical calls coincided with a movement display and were performed by  
9 juvenile individuals during solo singing (which allowed for isolation of the calls). Investigating  
10 these vocal-motor events, we found that body acceleration estimated using computer vision was  
11 statistically associated with the nearest peak in the amplitude envelope of the call, and that body  
12 acceleration timeseries contained mutual information about the amplitude envelope timeseries  
13 during these events. By confirming via quantitative methods that singing and movement are  
14 coordinated, the current report invites further mechanistic investigation on vocal-locomotor  
15 coupling in siamang.

16 *Keywords:* Siamang, Locomotor-vocal coupling, Locomotion, Respiration, Vocalization,

17 Multimodal Communication

## 1 Introduction

2 Human and non-human animals often coordinate whole-body movement with  
3 vocalizations. Multiple bat species (e.g., *Phyllostomus hastatus*) flexibly synchronize their echo-  
4 locating pulses with their wingbeats while flying, often in 1:1 or polyrhythmic fashion [1–4].  
5 Twelve species of North- and South-American birds show an allometrically coupled wingbeat  
6 duration with vocal unit durations [5]. Gerbils (*Meriones unguiculatus*) locomote in a saltating  
7 way, when they hop and hit the ground with their forelimbs they synchronously emit a  
8 vocalization [6]. The male brown-headed cowbird (*Molothrus ater*) uses vigorous wingbeats in  
9 courtship displays, and such activity affects respiratory-vocal activity [7]. Finally, humans also  
10 show synchronization of impulses of their limb movements with their vocalization (Pearson and  
11 Pouw, 2022; Pouw et al., 2020; Pouw et al., 2023; Serré et al., 2022; for an overview see Pouw  
12 and Fuchs, 2022).

13 Surprisingly, it is virtually unknown whether non-human primates synchronize their  
14 whole-body movements with vocalization. One taxon seems the perfect model to study vocal-  
15 motor interactions, building on anatomical and neural circuitry shared across primates, including  
16 us: the Gibbons and Siamang (*Hylobatidae*). They are highly vocal species and they load their  
17 entire body weight on their pectoral system during their primary mode of locomotion –  
18 *brachiation*. Here we focus on the heavier-weight Siamang (*Syndactylus syndactylus*).

19 Siamang and Gibbons diverge in several ways from great apes. They are a highly vocal  
20 species, performing extremely loud (sometimes > 100 Decibels [13,14], rhythmically  
21 coordinated songs [15], supporting family-bonding and territory-marking, and on occasion  
22 alarming. While usually understood as containing stereotyped vocalizations, Siamang song  
23 contain considerable variability for certain call phrases [16]. Siamang and Gibbons apes also  
24 move at extremely fast 45km/h speed using hand-over-hand grasps, also known as brachiation.  
25 These Small Asian Apes also move *while* they sing (e.g., [see here](#)). Interestingly, Haimoff  
26 (Haimoff, 1981), p. 135) observes a temporal coordination of locomotion and vocalization in the  
27 wild Siamang they studied. These and other widespread *qualitative* observations [18,19] suggest  
28 that singing in Siamang and Gibbons may at times be a combined display<sup>1</sup>, such that two

2 <sup>1</sup> Note that some Gibbon species (but not Siamang) are known to also dance outside of the context of singing [20],  
3 but that refers to a different sort of behavior.

1 behaviors (vocalization & movement) that in principle can operate alone, structurally operate  
2 together, much like other animals that move and vocalize in coordinated ways [1,5,7,21].  
3 However, no quantitative evidence exists to support the idea of a combined display. Perhaps in  
4 part because it is difficult to isolate calls often produced in group singing, and in part because  
5 movements of these apes are difficult to track – at present it seems virtually impossible to track  
6 movements of the Siamang in the wild as these apes move through the canopies with high speeds  
7 [22].

8 One interesting possible reason for vocal-motor coupling in Siamang is biomechanics. A  
9 range of animals that include their pectoral limbs for locomotion (e.g., bats, dogs, horses,  
10 rhinoceros) synchronize their locomotor cycles at increasing gait speeds with respiratory cycles  
11 [23]. This synchronization is held to occur because of a piston-like effect where the visceral  
12 organs push forward on the lungs during accelerations and decelerations of the body during  
13 locomotion strides (Daley et al., 2013; Lafortuna et al., 1996; for an overview see Pouw and  
14 Fuchs, 2022), or because muscle activation for locomotion driving movement accelerations  
15 simultaneously compress the rib-cage [1]. Interestingly, it has been generally acknowledged that  
16 brachiation in primates likely affects respiratory control and thus vocalization [26–29]. Thus  
17 from biomechanics of brachiation alone we would hypothesize some respiratory interactions,  
18 suggesting some potential for vocal-motor coupling. Other non-mutually exclusive hypotheses  
19 for coordination of voice and whole-body movements hold that combining visual and auditory  
20 signals increases the likelihood of communicative success [30,31].

21 In this study we opportunistically observed captive Siamang engaged in solo singing to  
22 assess vocal-motor coupling, whereby we audio-visually recorded singing for a period of 21  
23 days. We noticed characteristic vocalizations combined with pulse-like movements (e.g., for  
24 examples see [here](#)). These movement-accompanied calls contained ululating screams as main  
25 units [32] and were produced by juveniles who engaged in solo singing after the duetting  
26 singing performed by the entire group was completed or was winding down. To our surprise  
27 these specific stereotypical calls were *always* produced with a pulse-like movement. These pulse-  
28 like movements were seemingly synchronized with the calls and we will assess whether these  
29 movements associate with the loudness of these solo-songs in two analyses. We know from  
30 biomechanics in humans and other animals that the physical impact of a movement on the

1 musculo-skeletal system is during acceleration or deceleration (as forces are a function by mass  
2 [a constant] and acceleration) [6,9,24,25]. Therefore, we test here whether thorax accelerations  
3 during vocalizations statistically relate to the amplitude of concurrent vocalization in Siamang.

4

## 5 **Materials and methods**

### 6 **Data recording**

7 Audiovisual recordings of a family of Siamang (6 members; female adult, male adult,  
8 two male juveniles, one infant, and a newborn) were collected in the June and August of 2022  
9 over two visits at the Jaderpark Zoo in Lower Saxony, Germany. This yielded over 7 hours of  
10 recorded singing, collected by the first and second authors. The Siamang sang primarily in the  
11 morning around 9-10am, or after their fruit and vegetable lunchtime, around 1pm, and  
12 occasionally around 5pm. Only two juvenile/young adult individuals performed the stereotypical  
13 movement-accompanied vocalizations we consider here, and these events were ideal for acoustic  
14 analysis as there was no overlap compared to the typical collective singing of Siamang. Due to  
15 the adults and juveniles singing together, there is almost constant overlap in calls, which made us  
16 focus on the solo singing of the juveniles in this first investigation of siamang singing and  
17 movement. The two individuals were Baju (7 years and 8m) and Fajar (4 years and 11m). Baju  
18 and Fajar were both born in the Jaderpark zoo. During data collection, Baju was separated from  
19 the family due to risk of injury after a fight where all family members attacked Baju. This also  
20 means we could not collect *more* data from Baju during our second testing period as he was  
21 transferred to a smaller facility and stopped singing during our visit when the transfer was made.

### 22 **Audio-visual recording**

23 Four GOPRO Hero9 were installed, set at 1080 quality, sampling at 59.74fps, with linear  
24 lens settings. We then cropped frames and recompressed the video to 50fps. The camera  
25 positions were positioned as orthogonally from each other as the site allowed. Figure S1, panel a,  
26 shows a sketched map with geometrically estimated distances based on a laser-pointer  
27 measurement device. We further use in this study four audio sources from Sennheiser  
28 microphones with windjammers (MKE400), plugged into the GO-PRO ensuring audio-visual  
29 synchronization, sampling at 48kHz.

1 Recording was set at similar gains across microphones, and we checked for clipping  
2 during pilot recordings. The four acoustic waveforms were combined using an ‘Adobe Premiere  
3 Pro 2019 CC’ waveform alignment, which uses a cross-correlation approach to find the optimal  
4 lag to synchronize peaks in the audio. After synchronizing the waveforms of the four sources, we  
5 recompressed the audio as a single-channel audio source which thereby contains the combined  
6 time-aligned sources (48kHz). Therefore, we always estimate amplitude using four combined  
7 audio sources that collected from multiple locations to increase our measurement accuracy to  
8 track the sound’s amplitude. Specifically, we placed the audiovisual recorders at four different  
9 angles; this strategy minimized problems with differences in sound radiation and differences in  
10 sender-recording distances across different events, which may otherwise affect measurement of  
11 amplitude peaks. However, the amplitude measurements will be flawed in open environments  
12 such as these. For this reason, we also report a second time series analysis unaffected by  
13 differences in amplitude measurements across events (see lagged mutual information).

#### 14 **Identification of movement-accompanied vocalizations and related features**

15 The first and the second author identified opportunistically as many movement-  
16 accompanied vocalizations by going through all the recorded songs and annotating these events  
17 in ELAN [33]. These vocalizations were easy to identify because they all consisted of a ululating  
18 scream as a main unit, and any variability in the call structure was stereotypical within each of  
19 the two individuals. Interestingly, these stereotypical vocalizations always co-occurred with a  
20 pulse-like movement, though with variable intensity and different types of locomotion. The  
21 annotators (second and first author) drew a boundary around the movement-vocalization event,  
22 such that the movement and the vocalization sequence was contained. We will refer to these  
23 annotated events as movement-accompanied vocalizations throughout.

24 Importantly, we did not observe any stereotypical vocalizations that occurred with no  
25 observable movement at all (though some contained small amplitude movements, and these are  
26 part of the variability in our dataset; e.g., see supplemental table S1, Example 1). Please also see  
27 a longer segment of a juvenile’s singing in which it becomes clear that the stereotypical  
28 movement-vocal calls that comprise our data are embedded in other types of calls such as  
29 sequences of barks: see supplemental table S1, Example 2).

1 Also note that we focused on Juveniles because they would sing on their own. The adult  
2 female and male produced movement and vocalizations too. However, their movement-  
3 accompanied vocalizations almost always occurred when all individuals were singing. This lead  
4 to frequent, multiple overlaps. Analyses of overlaps that would require another set of acoustic  
5 post-processing steps that would greatly complicate the analysis relative to the current approach.

6 The degree of physical interactions expected are likely dependent on the type of action  
7 performed during vocalizations; therefore, we attempted to apply a standardized description to  
8 locomotor actions. We used Hunt's typology of locomotion types [34] to characterize the action  
9 that occurred during the vocalization (Figure 1). In some instances, we slightly deviated from  
10 Hunt's [35] categories to accommodate for a particular locomotion action (e.g., 'drop fore limb  
11 swing': the individual sits on top of horizontal structure, and then scoots backwards or forward to  
12 drop and then swing forward with two extended arms). A common mode of locomotion for  
13 Siamang, ricochet brachiation (e.g., see supplemental table S1, Example 3), is absent in our  
14 dataset, possibly due to the facility having more ropes than rigid and connected supports, and  
15 thus being more tailored towards swinging movements rather than ricochet brachiation. Some  
16 movement-accompanied vocalizations remained undefined as they did not fall into a clear  
17 category (i.e., mixed locomotion modes). We will make a crude binary distinction between  
18 locomotion types which load the entire weight on the thorax via the shoulder girdle(s) (forelimb  
19 only<sup>2</sup>), or those that involve distribution of weight or support via the lower limbs (other). In the  
20 case of forelimb only loads, one would particularly expect accelerations to constrain respiratory-  
21 vocal interactions.

22

### 23 **Video preprocessing and post-processing**

24 Each event can potentially be recorded via four camera angles. We first checked all these  
25 camera angles to see whether the individual was visible. If the individual was not visible, it was  
26 excluded as a potential camera angle submitted for analysis. Video processing was performed in  
27 Python, the specific steps discussed below. Further processing to prepare the dataset for  
28 statistical analyses was performed in R and R-studio.

---

2 <sup>2</sup> Strictly speaking, since siamang are primarily bipedal, we could have also referred to the pectoral limbs as upper  
3 limbs (rather than forelimbs). But we decided to follow Hunt's categories here.

1 **Cutting scenes and performing initial motion detection with OpenCv2.** Firstly, a2 custom Python script automatically cut the videos based on the ELAN annotations begin and end  
3 times using moviepy, ffmpeg and pydub (see supplemental table S1, Script 1).

4 Secondly, we determined regions of interest for each scene. The installed cameras had a

5 field of view to opportunistically capture behavior at different locations. This makes tracking  
6 with supervised computer vision more computationally costly as there may be many individuals  
7 moving in a complex structured site. As a pre-processing step we therefore created a Python  
8 pipeline (see supplemental table S1, Script 2) using OpenCv2 that determined pixel deviations  
9 from the median to ascertain a key area of movement per frame. After smoothing and obtaining  
10 maxima, this key area was used to determine a static bounding box that would further serve to  
11 crop the video to primarily contain the movement of the siamang and exclude the rest of the  
12 complex scene (for an example see Figure S1 panel b).13 **Kinematics**14 **Tracking DeepLabCut.** A convolutional neural network (Resnet-50) was trained using15 DeepLabCut (version 2)[36] with 250 hand-labeled frames (see Supplemental table S1, Resource  
16 1). Two key points were used for the training set. The first key point effectively tracked the upper  
17 thorax region targeted at the most posterior region (i.e., which was used for acceleration). The  
18 second key point was targeted at the sacrum of the individual (which was used for the body  
19 normalization of the acceleration magnitudes).

20 We trained the model with half a million iterations, reaching an average error rate of 1

21 pixel (for keypoints with 60% confidence rates) in the training set, and 25 pixels in the test set. If  
22 we normalize these errors by the original frame-sizes (1500x1080), then we get an error of  
23 0,0015%.

24 When using the trained model to extract position traces for the video recordings, we

25 applied the model to all events with DLC's native filtering option to remove noise-related jitter,  
26 yielding x,y position traces for the two key points (see Supplemental table S1, Example 4) and  
27 likelihoods. Since derivatives increase power of noise-related jitter relative to slower frequencies  
28 [37], we also applied extra smoothing of the resultant position traces with a 9th order  
29 Kolmogorov Zurbenko filter with a span of 110ms (R-package kza).

1        Likelihoods were further used for data quality curation. Specifically, if a camera angle  
2 had tracking that dropped for more than 5% below a threshold of .80, than we did not submit that  
3 particular camera for further analyses; the remaining 5% of the data, that had low confidences,  
4 were linearly interpolated (`na.approx` function using R-package `zoo`) using the surrounding  
5 high-confidence tracking samples. Note that the DLC team has recommended a likelihood of at  
6 least .60 for good tracking, and our pipeline is slightly more conservative than that.

7        **Normalization.** The thorax accelerations were calculated by differentiating speed  
8 measured in pixels over time. However, different camera positions, and different locations of the  
9 Siamang, make pixel-units problematic: a pixel as a unit of space will differ per distance of the  
10 camera to the individual. Therefore, we normalized the kinematics to a dimensionless quantity  
11 by scaling the position traces by the mean body size of the Siamang detected (for all frames that  
12 had a DeepLabCut confidence estimate of 100%). This means that all kinematics in this report  
13 are always first normalized by body size units.

14        **Approximating kinematics from multiple camera angles.** Depending on the location  
15 of the individual, we had one to four camera angles that recorded the movement-accompanied  
16 vocalizations. The many objects on the site, the distances of the cameras, the lack of access to the  
17 site, combined did not allow us to perform stereoscopic reconstruction of the camera angles to  
18 estimate 3D postures using a Charuco board [38,39]; this means the cameras could not be  
19 spatially calibrated for angle intrinsics and extrinsics. Note further that it would not be  
20 inappropriate to simply combine the 2D accelerations determined for each camera (by taking the  
21 Euclidean norm of all the 2D accelerations recorded) as this would yield an overestimation given  
22 that camera angles have correlated information (for example, because they all capture vertical  
23 acceleration of the individual). Therefore, to combine the information we need to find the non-  
24 correlated information in each of the camera views.

25        To still make use of multiple cameras (in the case when more than one camera had  
26 sufficient-quality data) that were impossible in the zoo to calibrate, we devised another solution  
27 to utilize multi-angle camera information using Principal Component Analyses (see e.g., [40],  
28 which formed the basis for our approximation of the 3D acceleration of the Siamang. We  
29 combined position traces of  $n$  cameras ( $c$ ) available  $\mathbf{M} = [x_{c=1}, y_{c=1}, x_{c=2}, y_{c=2} \dots x_{c=n}, y_{c=n}]$  to a  
30 principal component analysis, to calculate the eigenvectors ( $v$ ), where we extract the three

1 highest loading principal components,  $\mathbf{PC}_{1-3} = [\mathbf{Mv}(:,1), \mathbf{Mv}(:,2), \mathbf{Mv}(:,3)]$ , which will  
2 approximate positional information about orthogonal planes. Subsequently, we take the  
3 Euclidean norm of the derivatives of the first three principal components to get an approximation  
4 of 3D speed vector  $\mathbf{s}$ , such that  $\vec{s} = \sqrt{(\Delta PC_1)^2 + (\Delta PC_2)^2 + (\Delta PC_3)^2}$ . This norm is then differentiated  
5 once more, and absolutized, to yield an approximated 3D acceleration magnitude vector,  
6 ( $\vec{a} = |\Delta \vec{s}|$ ). Note after each differentiation we smooth the data with a 5th order Kolmogorov  
7 Zurbenko filter with a span of 50ms.

## 8 **Acoustics**

9 **Smoothed amplitude envelope.** We extracted a smoothed amplitude envelope of the  
10 waveform from the combined audio sources using a common approach, by first applying a  
11 Hilbert transformation [41], and then taking the complex modulus. This resulted in a one-  
12 dimensional time series, which was downsampled to 100Hz and further smoothed with a 12 Hz  
13 Hanning window.

## 14 **Aggregation of multiple data streams**

15 We synchronized the motion tracking data and the acoustic data by first aligning the data  
16 samples in time, and upsampling the motion tracking to 100Hz to preserve the high-sampling  
17 rate of the acoustics. We upsampled the motion tracking data by linearly interpolating the data  
18 along a time vector using R-package `zoo` (function `na.approx`; Zeileis and Grothendieck,  
19 2005) so as to have a regular sampling rate at 100Hz that exactly matches the sampling times of  
20 the amplitude envelope. This yields a combined time series with acoustics and motion tracking  
21 that could be further processed for analysis. R-code performing the above-mentioned processing  
22 steps is available online (see supplemental table S1, Script 3).

## 23 **Final processed dataset**

24 After having to exclude 29 events that had low-confidence tracking (trackings that  
25 dropped more than 5% below a threshold of 80% likelihood determined by DeepLabCut) the  
26 final dataset consisted of 83 events (of which; 26 Baju and 57 Fajar).

## 27 **Analysis 1: Peak analyses**

28 For each movement-accompanied vocal event we determined the global maximum in  
29 absolutized acceleration (max acc), i.e., the largest magnitude of either acceleration or

1 deceleration. Then we obtained the local maxima in the smoothed amplitude envelope, with a  
 2 `findpeaks` function using R-package `pracma`. This allowed us to select the magnitude of the  
 3 local peak in the envelope nearest to max acceleration. Since the acoustic and acceleration peak  
 4 data were long-tailed distributed, we log transformed the variables (which also improved model  
 5 fits), and z-normalized. As additional information, we also report change in amplitude in terms of  
 6 Decibels by scaling the raw envelope signal by  $dB = 10 \cdot \log_{10}(x)$ . This way, we can estimate  
 7 how body acceleration tends to increase the amplitude by a certain amount of dB.

## 8 Analysis 2: Lagged Mutual Information Analyses

9 We used the function `cmi` from R-package `mpmi`[43], to compute for each vocal-motor  
 10 event the continuous mutual information (cmi) at different lags, where cmi at some lag is defined  
 11 as  $I(X;Y)\tau$  in eq. 1:

$$13 \quad I(X;Y)\tau = \int \int p(x_{t-\tau}, y_t) \cdot \log \left( \frac{p(x_{t-\tau}, y_t)}{p(x_{t-\tau}) \cdot p(y_t)} \right) dx_{t-\tau} dy_t \quad (1)$$

14 where  $X_t$  is the z-normalized timeseries of body acceleration,  $Y_t$  is the z-normalized  
 15 timeseries of amplitude envelope, and  $\tau$  is a predefined lag capturing the time delay between the  
 16 two variables. Note, that the  $p(x, y)$  refers to the joint probability density function of  $X$  and  $Y$ ,  
 17 and  $p(x)$  and  $p(y)$  the marginal probabilities.

18 Mutual information thus provides an estimate of the information gained in  $Y$  given  $X$  (at  
 19 a particular time lag). This analysis helps uncover linear and non-linear covarying information  
 20 and temporal dependencies between body acceleration and amplitude envelope. By z-  
 21 normalizing the time series within each event, this analysis is not dependent on the relative  
 22 differences in absolute amplitude of the sound and movement between events, but rather is a test  
 23 of whether movement and sound within an event are mutually coupled.

24 **False random pair.** A strong comparison condition was constructed to determine  
 25 whether mutual information was higher in the observed time series relative to some baseline.  
 26 Lagged mutual information was produced by comparing the amplitude envelope with a randomly  
 27 simulated time series, together forming a *false random pair*. For each event comparison, the  
 28 simulated body acceleration time series had the same mean, standard deviation, and  
 29

1 autocorrelation as the original event's body acceleration time series (using an autoregressive  
2 integrated moving average, or ARIMA, procedure). We would expect that mutual information is  
3 lower in false random pairs relative to real paired movement-vocalization events.

4 **Main measures.** To summarize the data, we obtained the maximum observed mutual  
5 information between movement and sound for each event over the different lags (max mutual  
6 information). We also collected the lag at which the maximum mutual information was observed  
7 to understand whether movement is more predictive of sound or vice versa.

8

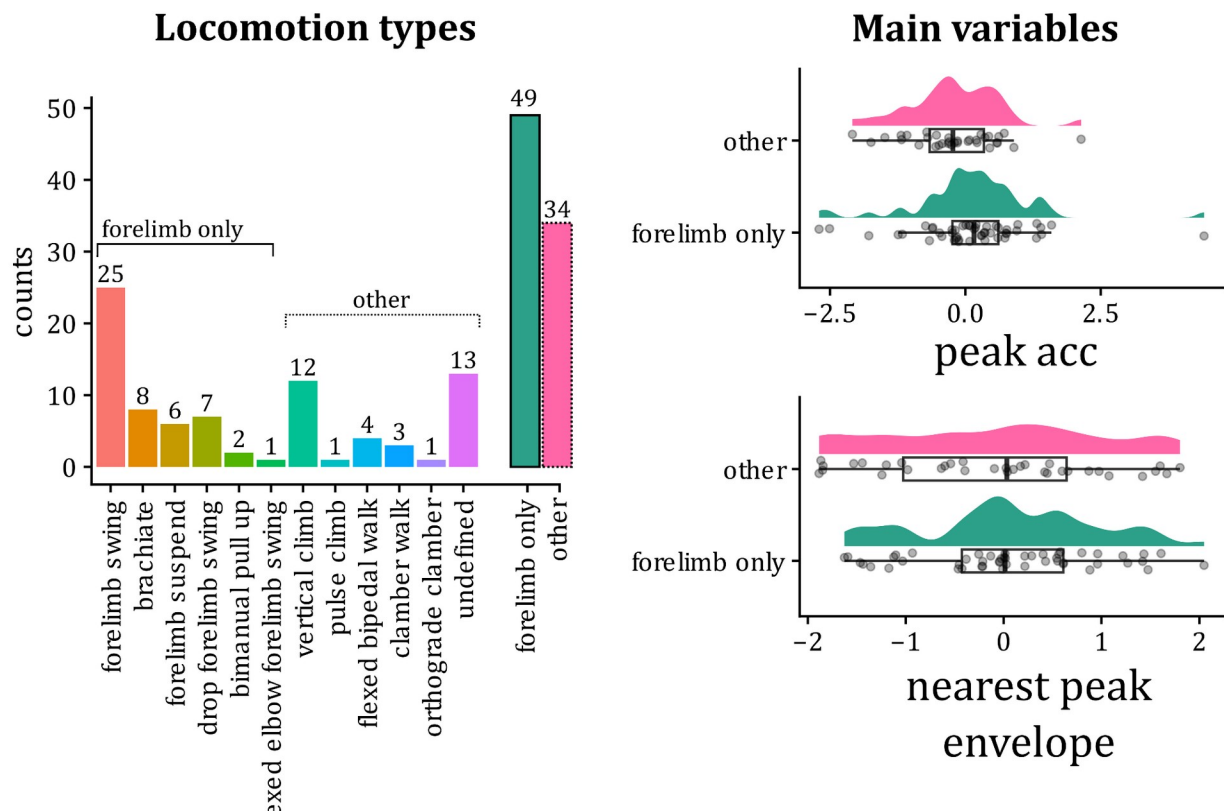
9 **Descriptive statistics**

10 An R markdown-script supporting the statistical analyses can be found online (see  
11 Supplemental table S1, Script 4). Figure 1 and Table S2 provide information about the main  
12 variables, as well as the time windows of the annotations (approximate length of the multimodal  
13 events). The temporal inter-peak distance between the global maximum in acceleration and the  
14 nearest local maximum in amplitude was on average 120 milliseconds ( $SD = 160$ ). This low  
15 temporal distance provides confidence that the two point-estimates for kinematics and acoustics  
16 occurred sufficiently close in time to be possibly coupled. Based on 95% confidence intervals,  
17 the older juvenile Baju seemed to generate higher peaks in the amplitude envelope (nearest to  
18 peak acceleration) as compared to his younger brother Fajar, while being comparable in their  
19 body accelerations peaks (see Table S2). Further, forelimb only locomotion tends to have higher  
20 accelerations than other locomotion types. The main variables did not dramatically differ either  
21 by individual or locomotion type.

22

23

1 **Figure 1. Frequency distributions for the locomotion types, peak acceleration, and limbs.**  
 2 The left panel shows the number of different locomotion types that we categorized for each  
 3 vocal-motor event. Since there are too many categories, with few instances, we created super  
 4 categories that indicate locomotion actions ( $N = 49$  forelimb only,  $N = 34$  for other types of  
 5 locomotion) that only included the fore/upper limbs (forelimb only), versus those that included  
 6 another limb (other). We use this super category to check whether our continuous kinematic-  
 7 acoustic analyses may give different results when we also consider what type of locomotor type  
 8 was performed. On the right panel, the distributions are shown for the magnitude (z-scaled units  
 9 per individual) in the global peak of acceleration, per binary locomotion category, showing for  
 10 example higher mean acceleration for forelimb only locomotor actions as opposed to other  
 11 actions that include the hindlimbs.



## Results and Discussion

12  
 13 To assess whether body accelerations constrain vocalizations amplitude, we assess  
 14 whether both parameters reliably scale in magnitude. Figure 2 provides a summary of the  
 15 procedure and the main results.

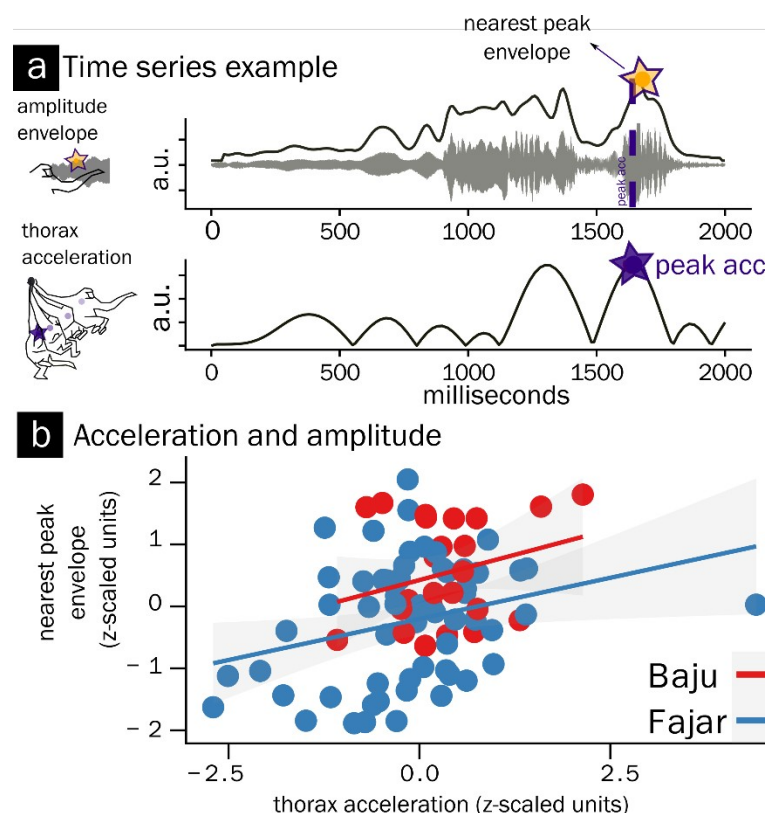
16 A mixed linear regression model was performed associating peak acceleration with  
 17 nearest peak of the call amplitude envelope (using maximum likelihood from R-package `n1me`;  
 18 Pinheiro et al., 2019). Individual (Fajar, Baju) was set as random intercept, but a model with

1 random slopes for individual did not converge. By setting Individual as random intercept we  
2 assess a relationship within individual, and we therefore do not simply lump together the data in  
3 establishing an association between body acceleration and amplitude envelope. The model  
4 statistically predicting peak envelope from peak acceleration reliably outperformed a base model  
5 predicting the overall mean in amplitude; change in  $\chi^2$  (1) = 7.68,  $p = .006$ . The model  
6 coefficients indicated that a higher magnitude peak in acceleration reliably associated with higher  
7 magnitude envelope peaks,  $b = 0.29$ ,  $b$  95%CI = [0.08, 0.49],  $t(80) 2.82$ ,  $p = .006$ , intercept  $b =$   
8 0.09,  $t(80) = 0.41$ ,  $p = 0.682$ . Since the models are performed on a log-log scale, we can  
9 interpret the coefficients as indicating that for a unit of increase in acceleration there is a 30%  
10 increase in the magnitude of the nearest peak envelope (i.e.,  $\frac{1}{3}$  power relationship). If we rescale  
11 the amplitude envelope to dB, and perform the same model we yield that per body scaled change  
12 in acceleration, there is an increase in the peak envelope of about 1.4dB,  $b = 1.43$ ,  $b$  95%CI =  
13 [0.043, 1.435],  $t(80) 2.82$ ,  $p = .006$  (see [supplemental online figure](#)). A simple regression  
14 analysis (which lumps the data together) yields a similar conclusion for the main effect of body  
15 acceleration,  $r = .33$ ,  $t(81) = 3.18$ ,  $p = .002$ . Also, note that if we remove the possible outlier  
16 shown in Figure 2 panel b (see [supplemental online figure](#) without outlier) the conclusions  
17 remain unchanged,  $r = .38$ ,  $t(80) = 3.1829$ ,  $p < .0001$ .

18 We explored possible confounds (e.g., number of camera angles available) or moderators  
19 (e.g., locomotion type) of this kinematic-acoustic coupling via interactions, but such interaction  
20 models were not reliably outperforming our main model,  $\chi^2$  (1) < 8.44,  $p$ 's > .21 (see  
21 [supplemental online figure](#)). These checks for confounds or conditional factors provide  
22 confidence that effects of acceleration and vocalization are stable among different measurement  
23 conditions, individuals, and locomotion types.

24 Thus, we can conclude that the magnitude of vocalization amplitude peaks that occur  
25 around moments when the thorax undergoes its maximum acceleration or deceleration is  
26 positively associated with the magnitude of that acceleration. For an inspection of the movement-  
27 accompanied vocalizations underlying figure 2 see our [dynamic data dashboard](#) (for code, see  
28 supplemental Table S1, Script 5).

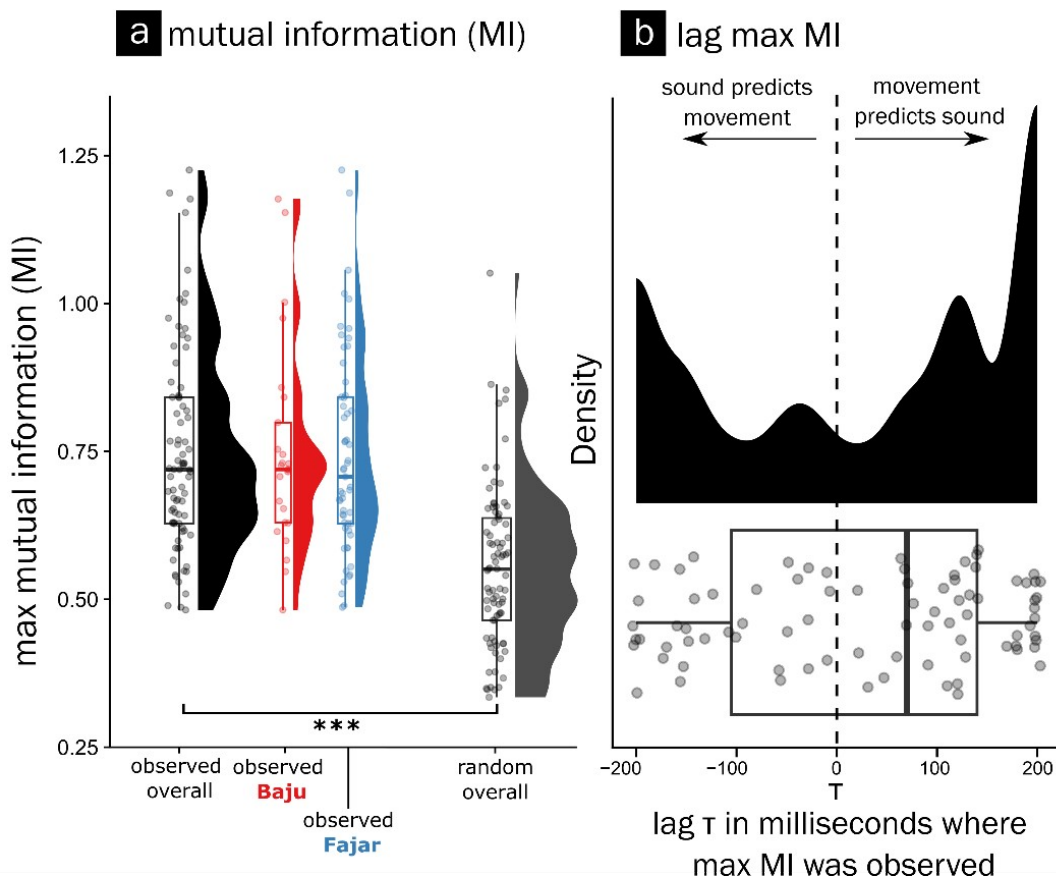
1 **Figure 2. Nearest peak analyses and results for acceleration and amplitude envelope** The  
 2 time series example (a) shows data for a single event (of 83 in total, 26 Baju and 57 Fajar). The  
 3 upper panel of (a) shows the smoothed amplitude envelope of the call; the lower panel of (a)  
 4 shows the acceleration of the thorax, both given in arbitrary units (a.u.). The purple star shows  
 5 the global maximum for acceleration. This maximum is then used to determine the nearest local  
 6 maximum in the amplitude envelope (yellow star, with purple outline), which in this case also  
 7 happens to be the global maximum in amplitude. The point-estimates are then submitted for  
 8 linear mixed regression with random intercepts for each individual, Baju and Fajar (b). Panel (b)  
 9 shows the nearest peak in body-scaled z-normalized thorax acceleration on the x-axis related to  
 10 the nearest z-normalized peak in the amplitude envelope on the y-axis (this relation was found to  
 11 be statistically reliable in a mixed regression analysis,  $p = .006$ ). See the [online dynamic](#)  
 12 [dashboard to explore the audiovisual data](#) underlying these data points which allows for  
 13 exploring each underlying audiovisual event.  
 14



15  
 16 While the peak magnitude analysis provides a promising indication that body  
 17 accelerations are associated with the loudness of the call, there is always a risk of unreliable  
 18 results given noisy amplitude measurement conditions, which may vary over the different  
 19 occasions the calls were produced. Therefore, we devised another test to statistically confirm an  
 20 association of movement and sound based on lagged mutual information calculations that assess  
 21 the continuous co-variance between two continuous variables. We assess mutual information at

1 different lags (-200 to +200 ms) in movement (body-scaled acceleration, z-normalized for each  
 2 event) and sound (amplitude envelope, z-normalized for each event). We set the lags at a  
 3 maximum of 200 milliseconds as any longer delays are unlikely to reflect a close coordination of  
 4 sound and movement (but rather some sequential organization). The lagged analyses allow for  
 5 possible coupling delays, indicating whether movement predicts sound in time rather than vice  
 6 versa.

7 **Figure 3. Mutual information between normalized movement and sound** a) The maximum  
 8 observed mutual information (in bits) in body acceleration and amplitude envelope over lags  
 9 from -200 milliseconds to 200 milliseconds is shown for observed movement-accompanied vocal  
 10 events (overall [N=83]; as well as split over individuals, Baju [N=26] and Fajar [N=57]) and  
 11 false random pair time series (random overall [N=83]). It is clear in a) that observed time series  
 12 have much higher mutual information than random pairs which was confirmed in a linear mixed  
 13 regression ( $p < .0001$ ), and it can be seen that Baju and Fajar show this high mutual information.  
 14 b) shows the lag at which the maximum mutual information is found for all actually observed  
 15 events as expressed in milliseconds. We obtain that relatively more often a maximum in mutual  
 16 information (MI) is found for when movement predicts sound in time, but our mixed regression  
 17 analyses did not find that a lag at max MI is reliably higher than 0ms ( $p = .08$ ).



1       A mixed linear regression model assessed whether the observed maximum mutual  
2 information is higher than a false random pair. Individual variability (Fajar, Baju) is accounted  
3 for as a random intercept (random slopes did not converge). A model contrasting a false random  
4 pair with the observed time series outperformed a model predicting the overall mean of mutual  
5 information,  $\chi^2 (1) = 54.49, p < 0001$ . The mutual information for false random pairs was indeed  
6 reliably lower than the observed mutual information,  $b = 0.20, b \text{ 95\%CI} = [-0.25, -0.15], t(163) -$   
7  $7.982, p < .0001$ . We further assessed whether the lags at which we obtained the max mutual  
8 information were reliably different from 0, thereby indicating that either sound or movement was  
9 predictive of the other in time. Though movement seemed more likely to be maximally  
10 predictive of sound at a lag between 0 to 200 milliseconds (see Figure 3) rather than the other  
11 way around, the intercept of a mixed regression model (with individual as random intercept)  
12 predicting the overall mean of the lag at max mutual information was not reliably different from  
13 0 with a two-sided test,  $b = +27\text{ms}, t (81) -1.80, p = .08$ . To conclude, we find clear additional  
14 evidence that there is mutual information in movement and sound, even if we ignore absolute  
15 measurements of sound and movement (as we z-normalize each time series per event). This  
16 report has therefore to remain inconclusive about whether movement predicts sound in time  
17 (though the data pattern toward movement predicting sound rather than vice versa).

18

19       The evolution of vocal production can be framed as a continuous stabilization of multiple  
20 interacting subsystems originally evolved for different purposes [45–49]. Many bodily systems  
21 must fall in line to produce such skilled and energetic vocal duet singing in Gibbons and  
22 Siamang. This duet singing is certainly shaped, as hypothesized till now, by several adaptations,  
23 such as complex vocal tract shaping [13] and the presence of laryngeal air sacs [50–52].  
24 However, here we show that that co-vocal movement and vocalization are mutually coupled in  
25 time and amplitude. We firstly obtain striking stereotypical pulse-like movements that co-occur  
26 with stereotypical vocalizations in two juvenile Siamang engaged in solo singing. In fact, these  
27 stereotypical vocalizations always occurred with (some) movements (few of these vocalizations  
28 occurred with very little movement, and these are included in our data, see the left region of the  
29 [dynamic plot to inspect the events with low body accelerations](#)). Using unsupervised and

1 supervised computer vision and data science methods we approximated the magnitude of peaks  
2 in 3D acceleration/deceleration of the thorax, which we then related to the magnitude of the peak  
3 in the smoothed amplitude envelope nearest to the moment of peak acceleration. We observed  
4 that the more the Siamang's thorax undergoes acceleration, the higher the amplitude of the  
5 vocalization, i.e., the louder the call. We further find that body accelerations are associated in  
6 time with changes in loudness, as established through finding higher mutual information of z-  
7 normalized movement and vocalization timeseries as compared against false pairs.

8 We speculate that the non-overlapping and loud solo songs may serve an 'honest  
9 signaling' function towards prospective mates (see e.g., Raemaekers et al., 1984). We would  
10 suspect that if these high-amplitude solo calls are designed to inform others about one's adaptive  
11 fitness, all available bodily resources will likely be recruited. This may mean that body  
12 movements stabilize and amplify said calls through some biomechanical cooperation (i.e., a  
13 synergy), or it may simply mean that more intense movements are coordinated as a visual display  
14 – a visual honest signal – that is coordinated with vocalization (i.e., a systematic combination of  
15 two signals). The current study merely shows an association between singing and movement, and  
16 more research is needed to understand the mechanisms and possible adaptive benefits of mutual  
17 coordination of song and movement.

18 Our results have several implications. Firstly, vigorous movements during singing in the  
19 Siamang have generally been described as combined 'movement *displays*'. However, our results  
20 suggest that these behaviors should also be understood as a coordination, where whole-body  
21 movement and sound combined in a structural way [9,30,31]. This further has essential  
22 implications for the large field of primate gesture studies, specifically as it tailors to the need for  
23 a better understanding of how different modalities contribute to communicative signaling [54,55]  
24 - after all, it seems that Siamang signal by using their body and their vocalization in a  
25 synchronized way. This synchrony reminds us of how professional human singers couple their  
26 upper limb movements during vocalizations [8]. It may be mechanistically analogous to how  
27 other non-human animals couple their pectoral limb activity to vocalization [1,5–7,23]. Our  
28 findings further tie in with recent research suggesting that species with more arboreal locomotion  
29 repertoires also have increased vocal singing abilities [56].

1 Importantly however, coupling of the respiratory-vocal system with peripheral bodily  
2 movements is not necessarily something that might drive vocal flexibility over evolutionary time  
3 [5,57]. Several avian vocal learners tend to have a looser allometric scaling of their wingbeat  
4 duration with their vocalization duration, as compared to birds who are not vocal learners [5].  
5 Mammalian vocal learners also tend to escape allometric scaling laws that relate vocalization and  
6 vocal tract size [58]. In humans, the increased flexibility in respiratory control has been in part  
7 attributed to a weakening of biomechanical constraint of locomotion with respiration (as the  
8 thorax was no longer impacted by locomotion; Bramble and Carrier, 1983). Furthermore, when  
9 mammals, including primates, need to do forceful activities that load onto the thorax, the glottis  
10 might need to be temporarily closed off to trap air to stiffen the thorax [6,9,27,59].

11 Thus, the possible functional interactions between locomotion and vocalization in  
12 primates is an open question. In avian species, for example, it has been shown that vocal  
13 development can be dependent on locomotor development [21,60]. Developmental research with  
14 marmoset monkeys has however shown that vocal development can occur even when locomotor  
15 development is delayed - Only an association of locomotor-postural development and vocal  
16 development was found (Gustison et al., 2019). Thus, more research is needed that not only  
17 assesses whether there is a link between locomotion and vocalization, but also how this then may  
18 play out over ontogenetic and evolutionary development.

19 There are several limitations to the current study. It is based on data from a single zoo  
20 obtained from captive juveniles, rather than wild adult Siamangs. It only considers certain  
21 vocalizations. These issues can only be resolved by collecting and analyzing more data and  
22 behaviors. Further, our measurements do not allow, at present, for more fine-grained 3D tracking  
23 of the animals as the cameras were impossible to calibrate at this zoo; the study setting also did  
24 not allow for perfect vocal amplitude measurements since that would require much more  
25 controlled parameters (e.g., the constant distance between source, the constant direction of  
26 radiation). We have reduced these issues through measuring from multiple directions and using  
27 signal processing techniques to obtain unique movement information from the cameras.

28 We should further highlight some of the hypothesized mechanisms that we put forward  
29 for vocal-motor interaction is on the level of biomechanics (kinematics) but our analyses and  
30 findings limited to kinematics, and accordingly more work is needed on the level of

1 biomechanics [1,22,62]. Such biomechanical work would need to evaluate how locomotion  
2 affects the surrounding respiratory system so that sub-glottal pressure increases due to some  
3 compression of the lungs. For example, activity of muscles that insert into the human rib cage  
4 (e.g., pectoralis major), measured via electromyography, predicts fluctuations in loudness in  
5 steady-state vocalizations during upper limb movements [11]. In Siamang similar but less  
6 invasive investigations could consist of measuring branch reaction forces during locomotion [22]  
7 and directly relating this to modulations in singing.

8 **Conclusions**

9 The potential coordination of singing with movement has fascinated gibbon researchers  
10 for a long time [17]. At the same time, current leading primatologists see the coordination of the  
11 voice and communicative movement as something that is not common in non-human primates  
12 [63]. The current report provides quantitative support that primate vocalization and whole-body  
13 movement is coordinating. Siamangs fluctuate their song amplitude together with body  
14 accelerations. They thus coordinate movement and singing in a way that is currently unknown.  
15 We hope therefore that this research further invites inquiry into the impressive movement-  
16 entangled vocalizations of Siamang and Gibbons.

17

18 **References**

- 19 1. Lancaster WC, Henson OW, Keating AW. Respiratory muscle activity in relation to  
20 vocalization in flying bats. *J Exp Biol.* 1995;198: 175–191.
- 21 2. Suthers RA, Thomas SP, Suthers BJ. Respiration, wing-beat and ultrasonic pulse emission  
22 in an echo-locating bat. *J Exp Biol.* 1972;56: 37–48.
- 23 3. Stidsholt L, Johnson M, Goerlitz HR, Madsen PT. Wild bats briefly decouple sound  
24 production from wingbeats to increase sensory flow during prey captures. *iScience.*  
25 2021;24: 102896. doi:10.1016/j.isci.2021.102896
- 26 4. Koblitz JC, Stilz P, Schnitzler H-U. Source levels of echolocation signals vary in  
27 correlation with wingbeat cycle in landing big brown bats (*Eptesicus fuscus*). *J Exp Biol.*  
28 2010;213: 3263–3268. doi:10.1242/jeb.045450
- 29 5. Berg KS, Delgado S, Mata-Betancourt A. Phylogenetic and kinematic constraints on avian  
30 flight signals. *Proc R Soc B Biol Sci.* 2019;286: 20191083. doi:10.1098/rspb.2019.1083

1 Amplitude of Vocalizations Associate with Body Accelerations in Siamang 21

1 6. Blumberg M. Rodent ultrasonic short calls: locomotion, biomechanics, and communication.  
2 J Comp Psychol. 1992;106: 360–365. doi:10.1037/0735-7036.106.4.360

3 7. Cooper BG, Goller F. Multimodal signals: enhancement and constraint of song motor  
4 patterns by visual display. Science. 2004;303: 544–546. doi:10.1126/science.1091099

5 8. Pearson L, Pouw W. Gesture–vocal coupling in Karnatak music performance: A neuro–  
6 bodily distributed aesthetic entanglement. Ann N Y Acad Sci. 2022;n/a.  
7 doi:10.1111/nyas.14806

8 9. Pouw W, Fuchs S. Origins of vocal-entangled gesture. Neurosci Biobehav Rev. 2022;141:  
9 104836. doi:10.1016/j.neubiorev.2022.104836

10 10. Pouw W, Paxton A, Harrison SJ, Dixon JA. Acoustic information about upper limb  
11 movement in voicing. Proc Natl Acad Sci. 2020 [cited 12 May 2020].  
12 doi:10.1073/pnas.2004163117

13 11. Pouw W, Werner R, Burchardt L, Selen L. The human voice aligns with whole-body  
14 kinetics. bioRxiv; 2023. p. 2023.11.28.568991.  
15 doi:<https://doi.org/10.1101/2023.11.28.568991>

16 12. Serré H, Dohen M, Fuchs S, Gerber S, Rochet-Capellan A. Leg movements affect speech  
17 intensity. J Neurophysiol. 2022 [cited 23 Sep 2022]. doi:10.1152/jn.00282.2022

18 13. Koda H, Nishimura T, Tokuda IT, Oyakawa C, Nihonmatsu T, Masataka N. Soprano  
19 singing in gibbons. Am J Phys Anthropol. 2012;149: 347–355. doi:10.1002/ajpa.22124

20 14. McAngus Todd NP, Merker B. Siamang gibbons exceed the saccular threshold: Intensity of  
21 the song of *Hylobates syndactylus*. J Acoust Soc Am. 2004;115: 3077–3080.  
22 doi:10.1121/1.1736273

23 15. Raimondi T, Di Panfilo G, Pasquali M, Zarantonello M, Favaro L, Savini T, et al.  
24 Isochrony and rhythmic interaction in ape duetting. Proc R Soc B Biol Sci. 2023;290:  
25 20222244. doi:10.1098/rspb.2022.2244

26 16. D'Agostino J, Spehar S, Abdullah A, Clink DJ. Evidence for Vocal Flexibility in Wild  
27 Siamang (*Sympalangus syndactylus*) Ululating Scream Phrases. Int J Primatol. 2023 [cited  
28 20 Sep 2023]. doi:10.1007/s10764-023-00384-5

29 17. Haimoff EH. Video Analysis of Siamang (*Hylobates syndactylus*) Songs. Behaviour.  
30 1981;76: 128–151.

31 18. Mitani JC. Gibbon Song Duets and Intergroup Spacing. Behaviour. 1985;92: 59–96.

32 19. Redmond J, Lamperez A. Leading limb preference during brachiation in the gibbon family  
33 member, *Hylobates syndactylus* (siamangs): A study of the effects of singing on  
34 lateralisation. Laterality. 2004;9: 381–396. doi:10.1080/13576500342000211

1 Amplitude of Vocalizations Associate with Body Accelerations in Siamang 22

1 20. Fan P-F, Ma C-Y, Garber PA, Zhang W, Fei H-L, Xiao W. Rhythmic displays of female  
2 gibbons offer insight into the origin of dance. *Sci Rep.* 2016;6: 34606.  
3 doi:10.1038/srep34606

4 21. Berg KS, Beissinger S, Bradbury J. Factors shaping the ontogeny of vocal signals in a wild  
5 parrot. *J Exp Biol.* 2013;216: 338–345. doi:10.1242/jeb.073502

6 22. Cheyne SM. Gibbon Locomotion Research in the Field: Problems, Possibilities, and  
7 Benefits for Conservation. In: D'Août K, Vereecke EE, editors. *Primate Locomotion:*  
8 *Linking Field and Laboratory Research.* New York, NY: Springer; 2011. pp. 201–213.  
9 doi:10.1007/978-1-4419-1420-0\_11

10 23. Boggs DF. Interactions between locomotion and ventilation in tetrapods. *Comp Biochem  
11 Physiol A Mol Integr Physiol.* 2002;133: 269–288. doi:10.1016/S1095-6433(02)00160-5

12 24. Daley MA, Bramble DM, Carrier DR. Impact loading and locomotor-respiratory  
13 coordination significantly influence breathing dynamics in running humans. *PLOS ONE.*  
14 2013;8: e70752. doi:10.1371/journal.pone.0070752

15 25. Lafortuna CL, Reinach E, Saibene F. The effects of locomotor-respiratory coupling on the  
16 pattern of breathing in horses. *J Physiol.* 1996;492 ( Pt 2): 587–596.  
17 doi:10.1113/jphysiol.1996.sp021331

18 26. Harrison DFN. *The anatomy and physiology of the mammalian larynx.* Cambridge:  
19 Cambridge University Press; 1995.

20 27. Hayama S. The origin of the completely closed glottis. Why does not the monkey fall from  
21 a tree? *Primate Res.* 1996;12: 179–206. doi:10.2354/psj.12.179

22 28. Mott F. A Study by Serial Sections of the Structure of the Larynx of *Hylobates syndactylus*  
23 (Siamang Gibbon). *Proc Zool Soc Lond.* 1924;94: 1161–1170. doi:10.1111/j.1096-  
24 3642.1924.tb03336.x

25 29. Negus VE. *The comparative anatomy and physiology of the larynx.* London: William  
26 Heinemann Medical Books; 1949.

27 30. Partan SR, Marler P. Communication Goes Multimodal. *Science.* 1999;283: 1272–1273.  
28 doi:10.1126/science.283.5406.1272

29 31. Halfwerk W, Varkevisser J, Simon R, Mendoza E, Scharff C, Riebel K. Toward Testing for  
30 Multimodal Perception of Mating Signals. *Front Ecol Evol.* 2019;7.  
31 doi:10.3389/fevo.2019.00124

32 32. Geissmann T. Duet Songs of the Siamang, *Hylobates Syndactylus*: II. Testing the Pair-  
33 Bonding Hypothesis during a Partner Exchange. *Behaviour.* 1999;136: 1005–1039.

34 33. Wittenburg P, Brugman H, Russel A, Klassmann A, Sloetjes H. *ELAN: a Professional  
35 Framework for Multimodality Research.* 2006; 4.

1 Amplitude of Vocalizations Associate with Body Accelerations in Siamang 23

1 34. Hunt KD. Why are there apes? Evidence for the co-evolution of ape and monkey  
2 ecomorphology. *J Anat.* 2016;228: 630–685. doi:10.1111/joa.12454

3 35. Hunt KD, Cant JGH, Gebo DL, Rose MD, Walker SE, Youlatis D. Standardized  
4 descriptions of primate locomotor and postural modes. *Primates.* 1996;37: 363–387.  
5 doi:10.1007/BF02381373

6 36. Mathis A, Mamianna P, Cury KM, Abe T, Murthy VN, Mathis MW, et al. DeepLabCut:  
7 markerless pose estimation of user-defined body parts with deep learning. *Nat Neurosci.*  
8 2018;21: 1281–1289. doi:10.1038/s41593-018-0209-y

9 37. Winter DA. Biomechanics and Motor Control of Human Movement. John Wiley & Sons;  
10 2009.

11 38. Karashchuk P, Rupp KL, Dickinson ES, Walling-Bell S, Sanders E, Azim E, et al. Anipose:  
12 A toolkit for robust markerless 3D pose estimation. *Cell Rep.* 2021;36: 109730.  
13 doi:10.1016/j.celrep.2021.109730

14 39. Theriault DH, Fuller NW, Jackson BE, Bluhm E, Evangelista D, Wu Z, et al. A protocol  
15 and calibration method for accurate multi-camera field videography. *J Exp Biol.* 2014;  
16 jeb.100529. doi:10.1242/jeb.100529

17 40. Mena-Chalco JP, Macêdo I, Velho L, Cesar RM. 3D face computational photography using  
18 PCA spaces. *Vis Comput.* 2009;25: 899–909. doi:10.1007/s00371-009-0373-x

19 41. He L, Dellwo V. Amplitude envelope kinematics of speech: Parameter extraction and  
20 applications. *J Acoust Soc Am.* 2017;141: 3582–3582. doi:10.1121/1.4987638

21 42. Zeileis A, Grothendieck G. *zoo: S3 Infrastructure for Regular and Irregular Time Series.* *J*  
22 *Stat Softw.* 2005;14: 1–27. doi:10.18637/jss.v014.i06

23 43. Pardy C. *mpmi: Mixed-pair mutual information estimators version 0.4 from R-Forge.* 2012.  
24 Available: <https://rdrr.io/rforge/mpmi/>

25 44. Pinheiro J, Bates D, DebRoy S, Sarkar D, R Team RC. *nlme: Linear and nonlinear mixed*  
26 *effects models.* 2019.

27 45. Pouw W, Proksch S, Drijvers L, Gamba M, Holler J, Kello C, et al. Multilevel rhythms in  
28 multimodal communication. *Philos Trans R Soc B Biol Sci.* 2021.  
29 doi:10.1098/rstb.2020.0334

30 46. Deacon TW. The symbolic species: The co-evolution of language and the brain. W.W.  
31 Norton; 1998.

32 47. Deacon TW. Incomplete Nature: How Mind Emerged from Matter. W.W. Norton; 2013.

1 Amplitude of Vocalizations Associate with Body Accelerations in Siamang 24

1 48. MacLarnon AM, Hewitt GP. The evolution of human speech: the role of enhanced  
2 breathing control. *Am J Phys Anthropol.* 1999;109: 341–363. doi:10.1002/(SICI)1096-  
3 8644(199907)109:3<341::AID-AJPA5>3.0.CO;2-2

4 49. MacNeilage PF. *The origin of speech.* Oxford University Press; 2010.

5 50. Burchardt LS, Sande Y van de, Kehy M, Gamba M, Ravignani A, Pouw W. A computer  
6 vision toolkit for the dynamic study of air sacs in Siamang with a general application to the  
7 study of elastic kinematics in other animals. 2023 [cited 15 Oct 2023]. Available:  
8 <https://ecoevrxiv.org/repository/view/6080/>

9 51. de Boer B. Acoustic analysis of primate air sacs and their effect on vocalization. *J Acoust  
10 Soc Am.* 2009;126: 3329–3343. doi:10.1121/1.3257544

11 52. Dunn JC. Sexual selection and the loss of laryngeal air sacs during the evolution of speech.  
12 *Anthropol Sci.* 2018;126: 29–34. doi:10.1537/ase.180309

13 53. Raemaekers JJ, Raemaekers PM, Haimoff EH. Loud Calls of the Gibbon (*Hylobates lar*):  
14 Repertoire, Organisation and Context. *Behaviour.* 1984;91: 146–189.

15 54. Liebal K, Slocombe KE, Waller BM. The language void 10 years on: multimodal primate  
16 communication research is still uncommon. *Ethol Ecol Evol.* 2022;0: 1–14.  
17 doi:10.1080/03949370.2021.2015453

18 55. Slocombe KE, Waller BM, Liebal K. The language void: the need for multimodality in  
19 primate communication research. *Anim Behav.* 2011;81: 919–924.  
20 doi:10.1016/j.anbehav.2011.02.002

21 56. Schruth DM, Templeton CN, Holman DJ, Smith EA. Evolution of primate protomusicality  
22 via locomotion. *bioRxiv*; 2021. p. 2020.12.29.424766. doi:10.1101/2020.12.29.424766

23 57. Bramble D, Carrier DR. Running and breathing in mammals. *Science.* 1983;219: 251–256.  
24 doi:10.1126/science.6849136

25 58. Garcia M, Ravignani A. Acoustic allometry and vocal learning in mammals. *Biol Lett.*  
26 2020;16: 20200081. doi:10.1098/rsbl.2020.0081

27 59. Orlikoff RF. Voice Production during a Weightlifting and Support Task. *Folia Phoniatr  
28 Logop.* 2008;60: 188–194. doi:10.1159/000128277

29 60. Liu W-C, Landstrom M, Cealie M, MacKillop I. A juvenile locomotor program promotes  
30 vocal learning in zebra finches. *Commun Biol.* 2022;5: 573. doi:10.1038/s42003-022-  
31 03533-3

32 61. Gustison ML, Borjon JI, Takahashi DY, Ghazanfar AA. Vocal and locomotor coordination  
33 develops in association with the autonomic nervous system. Tchernichovski O, Calabrese  
34 RL, Goller F, editors. *eLife.* 2019;8: e41853. doi:10.7554/eLife.41853

1 Amplitude of Vocalizations Associate with Body Accelerations in Siamang 25

1 62. Bertram JEA. New perspectives on brachiation mechanics. *Am J Phys Anthropol.* 2004;39:  
2 100–117. doi:10.1002/ajpa.20156

3 63. Fröhlich M, Sievers C, Townsend SW, Gruber T, Schaik CP. Multimodal communication  
4 and language origins: integrating gestures and vocalizations. *Biol Rev.* 2019;94: 1809–  
5 1829. doi:10.1111/brv.12535

6

1 **Supplemental materials**

## 2 Table S1. Links to online materials

Reference	Information	Hyperlink
Example 1	Example of data of small amplitude movements	<a href="#">link</a>
Example 2	Example of how stereotypical calls analyzed in this research are embedded in longer singing sequences	<a href="#">link</a>
Example 3	Example ricochet brachiation	<a href="#">link</a>
Example 4	Example of video tracking DeepLabCut	<a href="#">link</a>
Script 1	Python code for snipping videos from annotations	<a href="#">link</a>
Script 2	Python OpenCv2 automatic bounding box pre-processing script	<a href="#">link</a>
Script 3	R Processing script	<a href="#">link</a>
Script 4	R Statistical analysis	<a href="#">link</a>
Script 5	Python reproducible code for data dashboard	<a href="#">link</a>
Resource 1	Deeplabcut trained model + info	<a href="#">link</a>

3

4

5 Table S2. Descriptives stats main variables

Overall	Baju	Fajar	Forelimb only	Other
$M (SD)$	$M (SD)$	$M (SD)$	$M (SD)$	$M (SD)$
95%CI[]	95%CI[]	95%CI[]	95%CI[]	95%CI[]

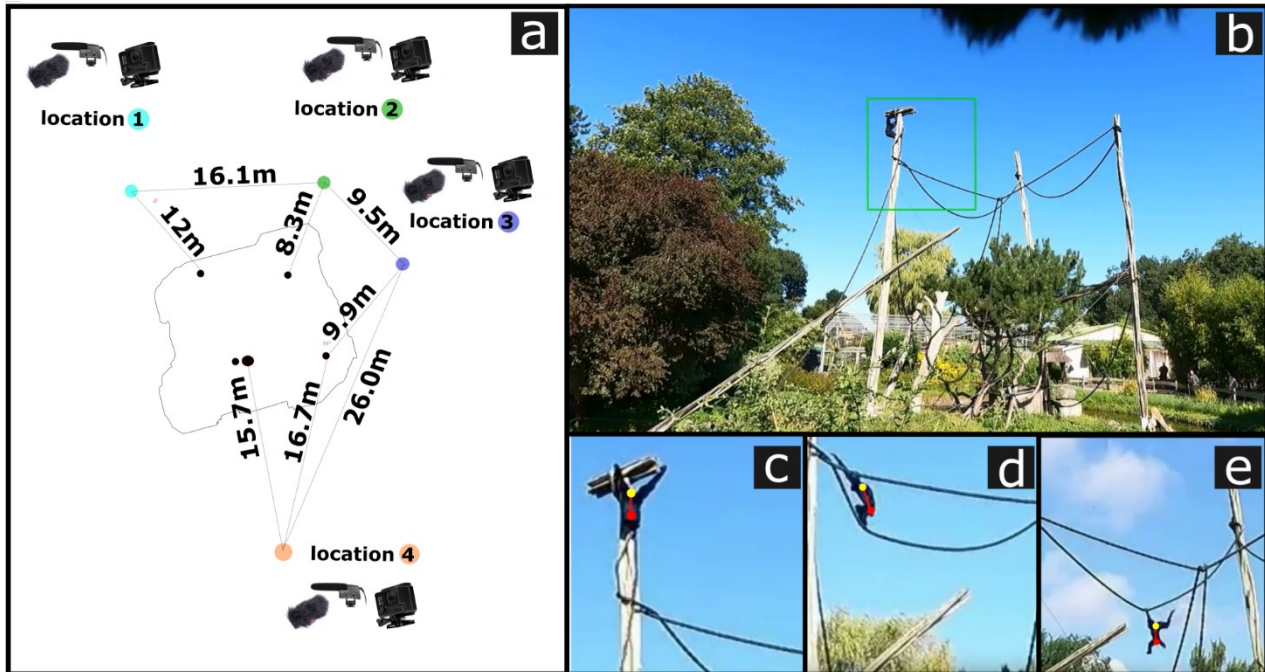
---

				
Time annotation	2851 ms (491) [2744, 2959]	2495 (268) [2386, 2603]	3014 (485) [2886, 3143]	2815 (485) [2675, 2954]
Nearest peak envelope ( $z$ )		0.52 (0.82) [0.19, 0.85]	-0.24 (.99) [-0.50, 0.03]	0.07 (0.91) [-0.19, 0.33]
Peak acceleration ( $z$ )		0.29 (0.69) [0.01, 0.57]	-0.13 (1.09) [-0.42, 0.16]	0.15 (1.09) [-0.21, 0.46]
Inter-peak distance	121 ms (160) [86, 156]	157ms (165) [90, 224]	104 (156) [62, 146]	107 (154) [62, 151]
1	Note. Max nearest envelope is the z-scaled magnitude of log peak smoothed amplitude envelope. Note that there are no overall descriptives for variables that have been z-scaled (amounting to $M = 0$ , $sd = 1$ ).			
2				

---

1 Note. Max nearest envelope is the z-scaled magnitude of log peak smoothed amplitude envelope. Note that there are  
2 no overall descriptives for variables that have been z-scaled (amounting to  $M = 0$ ,  $sd = 1$ ).

## 1 Figure S1. Keypoints tracked for different frames



2

3 Note. Panel a) shows a sketch of the location with four different recording sites with camera and microphones and  
 4 estimated distances obtained via laser-based distance estimation. b) Shows a frame from location 4 and an automatic  
 5 selection of the frame denoted by the green rectangle. c-d) These subframes containing movement in the frame were  
 6 then used for training DLC model to detect the two keypoints, shown in yellow (upper thorax, at T1) and red  
 7 (sacrum). The Euclidean distance of the upper thorax to the sacrum was used to normalize kinematics expressed in  
 8 pixel units to units relative to body size.

9

10